Investigation of nonlinear optical properties for laser dyes-doped polymer thin film

Ahmed A. Ali[1], Zainab F. Mahdi[2]
[1]Ministry of Science and Technolog, Iraq
[2]Institute of Laser for Postgraduate studies, University of Baghdad, Baghdad, Iraq
Email: Ahmed-alasady@yahoo.com

Abstract
Solutions of dyes Rhodamine 6G (Rh6G) and Coumarin480(C480) were prepared at five concentrations ($1x10^{-3}$, $5x10^{-4}$, $1x10^{-4}$, $5x10^{-5}$ and$1x10^{-5}$) mol/l, the mixing was stirred to obtain on a homogenous solution, the(poly methyl-methacrylate) (PMMA) was solved by chloroform solvent with certain ratio, afterward (PMMA+Rh6G) and (PMMA+C480) thin films were prepared by casting method on glass block which has substrate with dimensions (7.5 x2.5)cm^2, the prepared samples were left in dark place at room temperature for 24 hours to obtain uniform and homogenous thin films. UV-VIS absorption spectra, transmission spectra and fluorescence spectra were done to measure linear refractive index and linear absorption coefficient. The nonlinear optical properties of the prepared thin films were measured by z-scan technique. Two cases were measured: the first case is the closed-aperture z-scan to measure the nonlinear refractive index and the second case is open-aperture z-scan to measure the nonlinear absorption coefficient. The two cases were performed at two wavelengths 532 nm and 1064 nm and at two input fluences. For thin film (PMMA+ C480) the results show that the nonlinear absorption coefficient is directly proportional with the input fluence and directly proportional with increasing a concentration of the dye, while for thin film (PMMA+Rh6G) the nonlinear absorption coefficient inversely proportional with the input fluence and directly proportional with increasing a concentration of the dye. For thin films (PMMA+C480) and (PMMA+Rh6G) the nonlinear refractive index is inversely proportional to the input fluence. For both thin films the nonlinear absorption coefficient is more affected at wavelength 1064 nm and the nonlinear refractive index is more affected at wavelength 532nm.

Key words
Rhodamine 6G, Coumarin480, nonlinear optical properties

Article info
Received: Mar. 2010
Accepted: Dec. 2012
Published: Dec. 2012

دراسة الخواص البصرية اللاخطية لطبقة رقيقة من البوليمر المطعم بالصبغات الليزرية

أحمد عبد الزهرة علي[1] ، زينب فاضل مهدي[2]
[1]وزارة العلوم والتكنولوجيا، العراق
[2]معهد الليزر للدراسات العليا، جامعة بغداد، العراق

الخلاصة
في هذا الجزء العملي أستخدمت طريقة حديثة تعرف بتقنية المسح على المحـــــور الثالث (z-Scan) لدراسة الخواص البصرية اللاخطية مثل معاملات الانكسار والامتصاص اللاخطية لأفلام بولي مثيل ميثا اكريلات المطعمة بالصبغات الليزرية . تم تحضير محلـــــول كـــــل صبغة بخمسة تراكيز 1×10^{-3} , 5×10^{-4} , 1×10^{-4} , 5×10^{-5} ,1×10^{-5} مولاري، ثم تم اذابة حبيبات من بولي مثيل ميثا اكريلات بواسطة مذيب الكلوروفورم بنسبة معينة ، بعد ذلك يتم اضافة كمية مناسبة من محلول كل تركيز الى كمية مناسبة من محلول بولي مثيل ميثا اكريلايت ثم يرج المزيج بصورة جيدة لحين الحصول على محلول متجانس ، بعدها تتم عملية تحضير أغشية رقيقة من هذا المزيج وذلك بطريقة الصب على قالب زجاجي ذو

أرضية أبعادها (7.5 سم x 2.5 سم) موضوع على سطح مستو ثم تترك النماذج المحضرة في مكان مظلم وبدرجة حرارة المختبر لمدة 24 ساعة للحصول على تركيب متجانس ومنتظم للغشاء.

ولغرض التعرف على خصائص العينة تم اجراء عدة فحوصات مختبرية حيث تم اجراء فحوصات بصرية مثل فحص الامتصاصية والنفاذية والفلورة، حيث أجريت حسابات لقياس معاملات الانكسار والامتصاص الخطية بواسطة النفاذية ، ومن ناحية اخرى تم قياس السمك للأغشية الرقيقة باستخدام طريقة تداخل الأهداب ليكون بمعدل 7 مايكروميتر.

الخواص البصرية اللاخطية للأفلام البوليمرية قيست بواسطة تقنية المسح على المحور الثالث باستخدام ليزر النيديميوم-ياك النبضي وعند الطولين الموجيين 1064 نانوميتر، 532نانوميتر وعند كل طول موجي تم اجراء التجربة بحالتين: الحالة الأولى بوضع ثقب ضيق أمام الكاشف لغرض قياس معامل الانكسار اللاخطي والحالة الثانية بتكبير فتحة الثقب لغرض دراسة معامل الامتصاص اللاخطي. تم اجراء حالتي التجربة عند الطولين الموجيين 1064نانوميتر و 532 نانوميتر وبقيمتين للطاقة الداخلة، حيث بينت التجارب بأن معامل الامتصاص اللاخطي يتناسب طردياً مع زيادة الطاقة الداخلة وطردياً مع زيادة تركيز الصبغة بالنسبة للغشاء البوليمري المطعم بصبغة الكومارين C480، وعكسياً مع زيادة الطاقة الداخلة وعكسياً مع زيادة تركيز الصبغة بالنسبة للغشاء البوليمري المطعم بصبغة الرودامين Rh6G وهذا السلوك اللاخطي يكون اكثر تأثيراً عند الطول الموجي\1064 نانوميتر من 532نانوميتر .

معامل الانكسار اللاخطي يتناسب عكسياً مع زيادة الطاقة الداخلة وعكسياً مع زيادة تركيز الصبغات بالنسبة للغشاء البوليميري المطعم بصبغة الكومارين C480 والغشاء البوليمري المطعم بصبغة الرودامين Rh6G وهذا السلوك اللاخطي يكون أكثر تأثيرا عند الطول الموجي 532 نانوميتر من 1064 نانوميتر وأكثر تأثيراً في الأغشية الرقيقة المطعمة بصبغة الكومارين C480 من الأغشية الرقيقة المطعمة بصبغة الرودامين Rh6G .

Introduction

In a solid-state dye laser the organic dye molecules are uniformly distributed in a highly homogenous polymer matrix. An example of such polymer is a highly pure form of poly (methyl-methacrylate) (PMMA). Solid state dye lasers that span from the ultraviolet to the near infrared regions have been successfully demonstrated, photo stability of laser dyes in solid matrices remains an issue for continuous study [1]. An important feature of the dye laser is easily tunable over a wide range of wavelengths. Fluorescent dyes play an important role for staining and sensoring in analytical chemistry, environmental science, biology and medicine [2]. Some fluorescent dyes are used in dye lasers as active media [3]. To understand the nonlinear properties of fabricated laser dye-doped polymer thin films, there are several techniques have been used to measure nonlinear refractive index and nonlinear absorption coefficient including, z-scan, four-wave mixing[4]. The z-scan method provides a simple and straightforward method for the determination of the nonlinear refractive index and the nonlinear absorption coefficient. The technique has been widely employed for characterizing the optical nonlinearity of thin films. The simplicity of both the experimental setup and the data analysis has allowed the z-scan method to become widely used by many research groups [5, 6]. The Z-scan technique is a simple and popular experimental technique to measure intensity dependent nonlinear susceptibilities of materials. In this method, the material sample is moved in the z-direction along the axis of a focused Gaussian beam, and the far field intensity versus sample position Z-scan curve, predicated on a local response, gives the real and imaginary part of third order susceptibility. In this technique the optical effects can be measured by translating a sample in and out of the focal region of the incident laser beam. Consequently increases and decreases in the maximum intensity incident on the sample produces wave front distortions created by nonlinear optical effects in the sample along a well-defined, focused laser beam, and thereby varying the light intensity in the sample, by varying the aperture in the front of the detector, one

makes the Z-scan transmittance more or less sensitive to either the real or imaginary part of the nonlinear response of the material, i.e., nonlinear refractive index and nonlinear absorption, respectively. The Z-scan method is an experimental way to obtain data regarding the nonlinear refractive index and nonlinear absorption properties of materials. Here nonlinearity means the intensity dependent response of the material, which can be use to obtain an optical limiting device, either by nonlinear refraction or absorption [7, 8].

Nonlinear Absorption and Nonlinear Refraction

The basic optical properties involved in the light-matter interaction are absorption, which is defined by the absorption coefficient α, and refraction, which is defined by the index of refraction n. When the material is irradiated, the energy of the absorbed photons makes it possible for the transition from the ground state to the excited state. This process is called linear absorption. The further excitation may be possible due to the abundance of incoming photons; this process is called nonlinear absorption. The absorption of the material – α- is intensity dependant given by [9, 10]

$$\alpha=\alpha_o+\beta I \quad (1)$$

where, I : is the light intensity (or power density) , β: the nonlinear absorption coefficient related to the intensity, α_o : linear absorption coefficient.

There is also a change in the refractive index when a material is placed in a strong electric field. In fact, the index of refraction becomes dependant on the intensity of the electric field. At high intensity, the refractive index is given by [9, 10]:-

$$n=n_o+n_2 I \quad (2)$$

where, n_2: the nonlinear refractive coefficient related to the fluence,
n_o : linear refractive index.

A- Z-Scan Technique

There are two parts in z-scan process, the closed-aperture and open-aperture.

A1- Closed-Aperture z-Scan: A closed-aperture z-Scan measures the change in the intensity of a beam, focused by lens *L as* in Fig.1, as the sample passes through the focal plane. Photo-detector *PD* collects the light that passes through an axially centered aperture *A* in the far field. The focused beam has greatest intensity at the centre and will create a change in index of refraction forming a lens in a nonlinear sample as shown in Fig.1 [11].

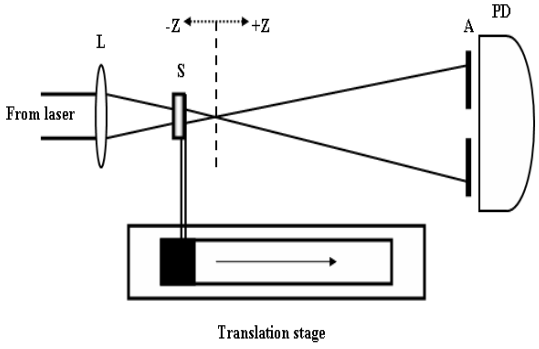

Fig. (1) Closed-aperture Z-Scan

The relative on-axis transmittance of the sample measured (at the small aperture of the far-field detector) is given by [7]:-

$$T_{(z,\Delta\Phi o)} = -1 \frac{4\Delta\Phi o\, Z/Zo}{[(Z^2/Zo^2)+9][(Z^2/Zo^2)+1]} \quad (3)$$

where, T is the transmittance through the aperture, which is a function of the sample position Z and nonlinear phase shift $\Delta\Phi o$, Z_o = the diffraction length, the nonlinear refractive index is calculated from the peak to valley difference of the normalized transmittance by the following formula [7]:-

$$n_2 = \Delta\Phi o / I_o L_{eff}\, k \quad (4)$$

where, $\Delta\Phi o$: nonlinear phase shift, $k = 2\pi/\lambda$, λ : is the wavelength of the beam. I_o is the intensity at the focal spot. L_{eff} : the effective

length of the sample, can be determined from the following formula [7]:

$L_{eff}=(1-e^{-\alpha oL})/\alpha_o$ (5)

where, L : the sample length,

The intensity at the focal spot is given by [7]:

$I_o=2P_{peak}/\pi\omega_o$ (6)

where, ω_o: the beam radius at the focal point, P_{peak} :- the peak power given by [12]:

$P_{peak}=E/\Delta t$ (7)

where, E : the energy of the pulse, Δt: the pulse duration.

A2- Open-Aperture z-Scan

An open-aperture z-Scan measures the change in the intensity of a beam, focused by lens *L as* in Fig.2, in the far field at detector *PD*, which captures the entire beam.

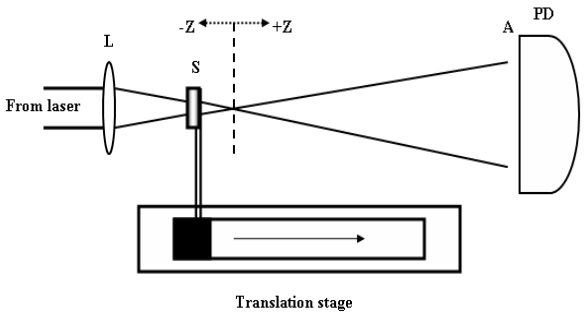

Fig. 2: Open-aperture Z-Scan

The coefficients of nonlinear absorption can be easily calculated from such transmittance curves [7]: The total transmittance is given by[7]:

$$T(z)=\sum_{m=0}^{\infty}\frac{\left[\frac{\beta I_o L_{eff}}{1+(Z/Zo)^2}\right]^m}{(m+1)^{3/2}} \quad (8)$$

where, *Z:* - is the sample position at the minimum transmittance, *m* :- integer. *T(z)*:- the minimum transmittance. The two terms in the summation are generally sufficient to determine the nonlinear absorption coefficient β.

Experimental

A - Solutions preparation

Solutions of concentration $1x10^{-3}$ M for each Rh6G and C480 in chloroform solvent were prepared. The powder is weighting using an electronic balance type (BL 210 S) Germany having a sensitivity of four digits.

Different concentrations were prepared according to the following equation:

$$W=\frac{M_W\ x\ V\ x\ C}{1000} \quad (9)$$

where

W weight of the dissolved dye (gm)

M_w molecular weight of the dye (gm/mol)

V the volume of the solvent (ml)

C the dye concentration (mol/l)

The prepared solutions were diluted according to the following equation:-

$C_1\ V_1 = C_2\ V_2$ (10)

where

C_1 primary concentration

C_2 new concentration

V_1 the volume before dilution

V_2 the volume after dilution

Five concentrations were prepared for Rh6G and C480.The concentrations are $1x10^{-3}$, $5x10^{-4}$, $1x10^{-4}$, $5x10^{-5}$ and $1x10^{-5}$ Molary

B - Fabrication of dye –doped polymer films

Dye doped polymer films were fabricated by casting block method. The solution of the polymer is prepared by dissolving the required amount of polymer (7 g in 100 ml of solvent). A required amount of dye solution was added to polymer solution and stirred at room temperature to get a uniform mixture. The polymer films were cast by allowing the mixed polymer solution to dry on a glass block has substrate with dimensions (7.5 x2.5) cm^2.

Process of solutions mixing and their ratios were performed for each concentration of a dye-doped polymer as the following:-

C480 + PMMA

Rh6G + PMMA

C- Sample Testing

Transmission, Absorption and Thickness Measurement

The prepared samples were tested using UV-visible spectrophotometer for measuring the transmission and absorption. The thickness of thin film was measured by Michelson interferometer.

Fluorescence measurements

SL 174 spectrofluorometer from optimize company (Japan) was used to test the fluorescence spectra of Rh6G & C480.

Z-scan System

Closed and open aperture z-scan measurements were. Each part was employed at 1064 nm and 532 nm. Fig.3 shows the set-up of the z-scan system.

Results and Discussion

Sample Testing

The linear optical properties of polymer film

Thickness Measurement: Using Michelson interferometer the film thickness is equal to 7μm.

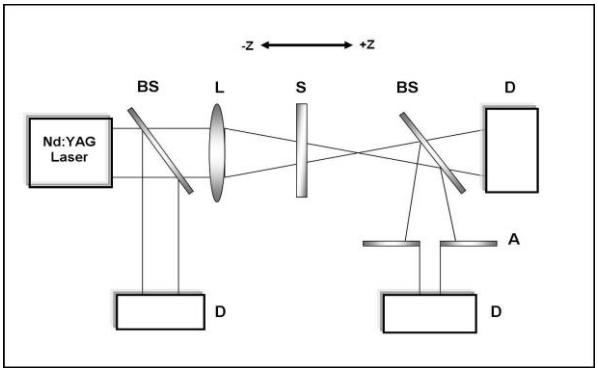

Fig.3: The set-up of Z-Scan system

BS:-beam splitter, L:-Lens, S:-Sample,
D:-Detector, A:-Aperture.

UV-VIS absorption spectra of polymer films

UV-VIS absorption spectra were obtained for a PMMA thin film. The behavior is shown in Fig.4. The absorption peak of PMMA thin film equals 375nm.

PMMA in chloroform

UV-VIS absorption spectra for PMMA after the addition different concentrations Rh6G dye the absorption peaks for (PMMA+Rh6G) films are 529, 530, 532, 533 and 535nm respectively,

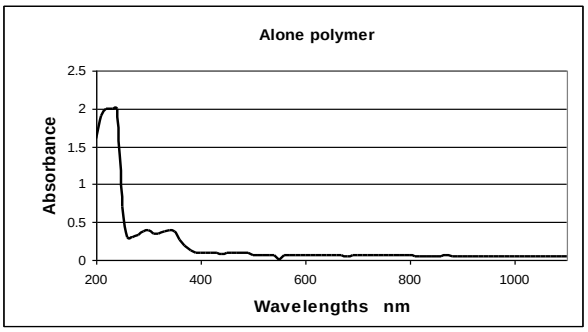

Fig.4: The absorption spectrum of the alone

while the absorption peaks for (PMMA+C480) films are 301,345,348,363 and 382nm respectively. The present results show that the absorption peaks for PMMA after adding different concentrations of Rh6G or C480 in chloroform solvent were shifted toward the longer wavelengths with increasing concentrations. This shift obtains due to increasing number of molecules per volume unit at high concentrations, this in turn lead to change in energy levels result in effect of vibration field on molecules.

Transmission spectra of PMMA films

The transmission spectra of the samples' film were analyzed using UV-VIS spectrophotometer. Fig.5 shows the transmission spectrum of PMMA.

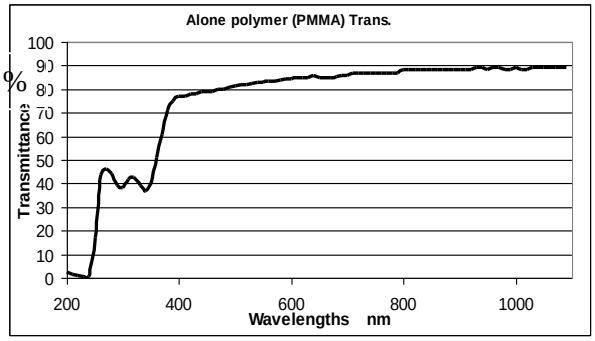

Fig.5: The transmission spectrum of the PMMA in chloroform

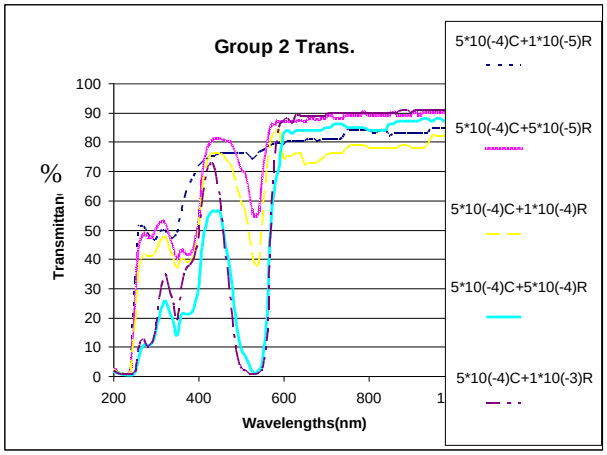

Fig.6: The transmission spectrum of the PMMA-dye with different concentrations of Rh6G

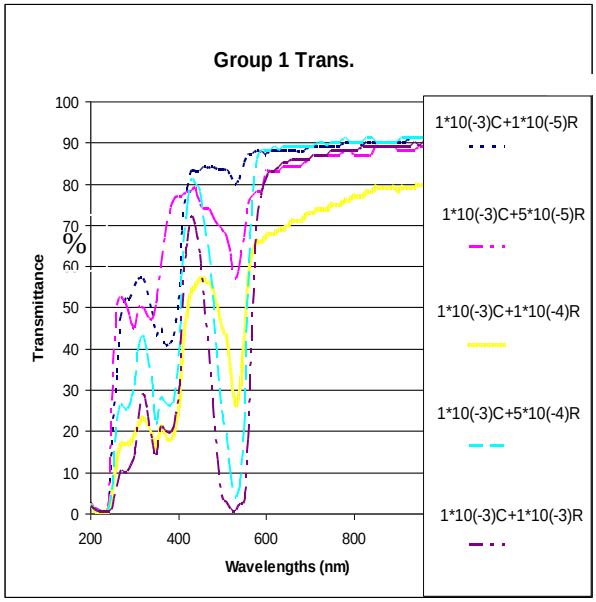

Fig.7: The transmission spectrum of the PMMA-dye with different concentrations of C480

The optical transmission of the films sample is shown a variable behavior of the transmission as a function of the incident wavelength. At the wavelength 532 nm the transmission behavior of PMMA is about 84%. While for PMMA with different concentration of Rh6G $1*10^{-5}$,$5*10^{-5}$,$1*10^{-4}$, $5*10^{-4}$ and $1*10^{-3}$ m/l the transmission behavior is 46, 34, 28, 1.6 and 0.5% respectively. At the wavelength 1064 nm the transmission behaviors of PMMA are about 90%. While for PMMA with different concentrations of Rh6G $1*10^{-5}$, $5*10^{-5}$, $1*10^{-4}$, $5*10^{-4}$ and $1*10^{-3}$ m/l the transmission behavior is 90, 88, 80.3, 68.4 and 80.7% respectively. Fig 7 shows the transmission spectrum of the PMMA-dye with different concentrations of C480. At the wavelength 532 nm the transmission behavior of PMMA with different concentrations of C480 $1*10^{-5}$, $5*10^{-5}$, $1*10^{-4}$, $5*10^{-4}$ and $1*10^{-3}$M the transmission behaviors are (79.4 ,78.8, 76.8, 73 and 68%) respectively. At the wavelength 1064 nm the transmission behavior of PMMA with different concentrations of C480 $1*10^{-5}$, $5*10^{-5}$, $1*10^{-4}$, $5*10^{-4}$ and $1*10^{-3}$ m/l the transmission behaviors are 88, 87.5, 87.3, 86.3 and 83% respectively.

Fluorescence spectra of PMMA films

Fig.8 shows fluorescence spectrum of alone PMMA film and Fig.9-13 show fluorescence spectra of Rh6G doped PMMA films at concentrations $1*10^{-5}$, $5*10^{-5}$,$1*10^{-4}$, $5*10^{-4}$ and $1*10^{-3}$M respectively:

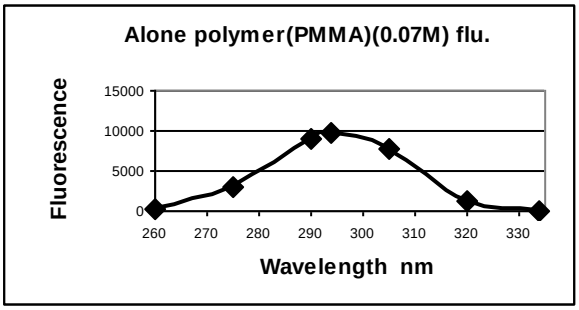

Fig.8: Fluorescence spectrum of alone PMMA film

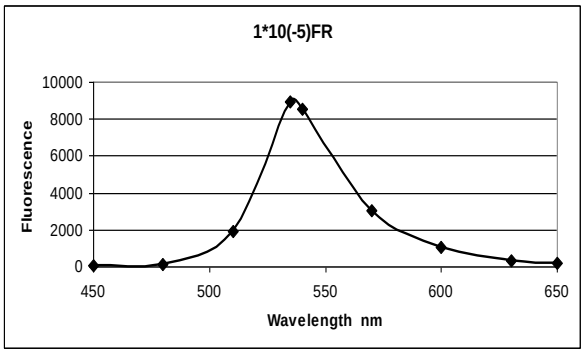

Fig.9: Fluorescence spectrum of PMMA film at $1*10^{-5}$ Rh6G

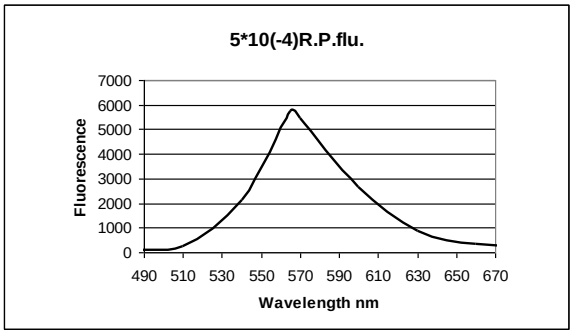

Fig. 10: Fluorescence spectrum of PMMA film at 5*10^{-5} Rh6G

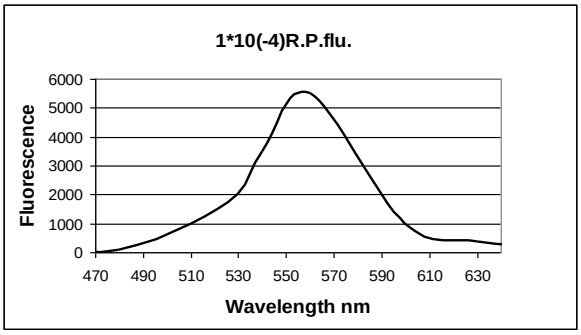

Fig.11: Fluorescence spectrum of PMMA film at 1*10^{-4} Rh6G

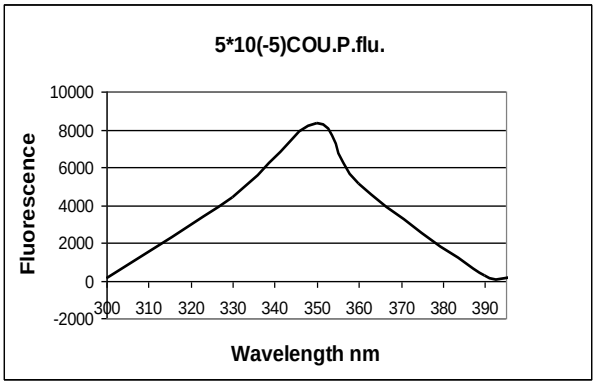

Fig. 12: Fluorescence spectrum of PMMA at

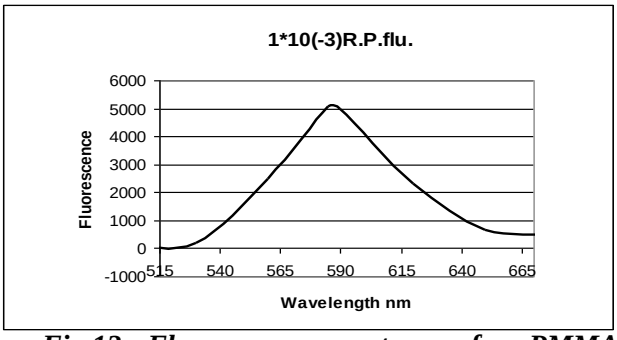

Fig.13: Fluorescence spectrum of PMMA film at 1*10^{-3} Rh6G

In Figs. 9-13 examination of these spectra indicated that the emission peaks shift to longer wavelength (red shift) with increasing concentration. This shift obtain due to increasing number of molecules per volume unit at high concentrations, this in turn lead to change in energy levels because effect of vibration field on molecules.

This concentration quenching is due to formation of dimers or other quenching complexes which have very fast radiationless deexcitation channels. Increasing concentration of Rh6G from $1*10^{-5}$M to $1*10^{-3}$M lead to broadening of fluorescence band from 100nm to 150nm.

Figs.14-18 show fluorescence spectra of C480 doped PMMA films at concentrations $1*10^{-5}$,$5*10^{-5}$,$1*10^{-4}$, $5*10^{-4}$ and $1*10^{-3}$M respectively:

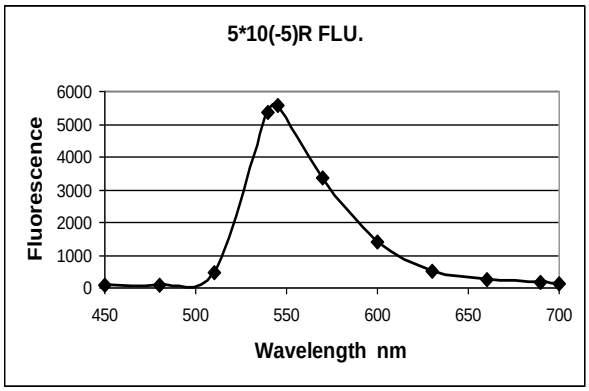

Fig.14: Fluorescence spectrum of PMMA film at 5*10^{-5} C480

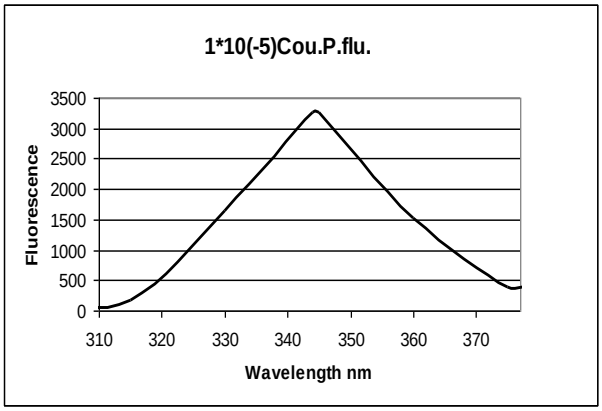

Fig.15: Fluorescence spectrum of PMMA film at 1*10^{-5} C480

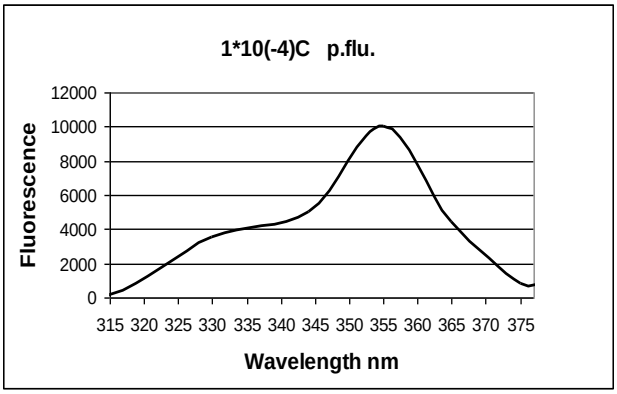

Fig. 16: Fluorescence spectrum of PMMA film at $1*10^{-4}$C480

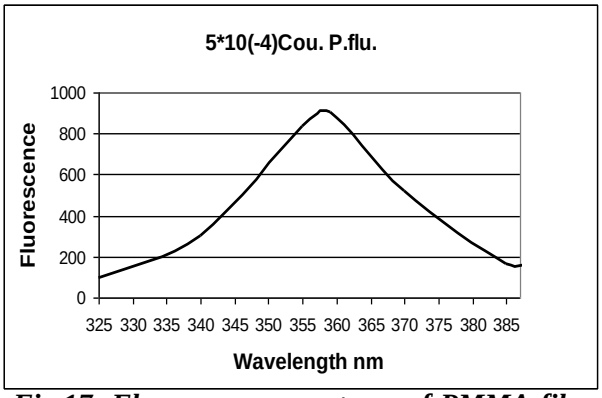

Fig.17: Fluorescence spectrum of PMMA film at $5*10^{-4}$ C480

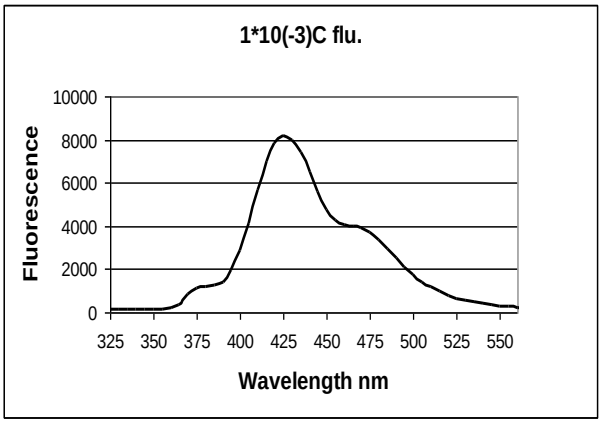

Fig.18: Fluorescence spectrum of PMMA film at $1*10^{-3}$ C480

In Figs.14-18 examination of these spectra indicated that the emission peaks shift to longer wavelength (red shift) with increasing concentration. The obtained shift was due to increasing number of molecules per volume unit at high concentrations, this in turn lead to change in energy levels because effect of vibration field on molecules. Increasing concentration from $1*10^{-5}$M to $1*10^{-3}$ M lead to broadening of fluorescence band from 70nm to 225 nm corresponding it observed reduction in intensity due to behavior part of dye molecules as quenching. Higher intensity was at concentration $1*10^{-4}$M of C480[13].

The nonlinear optical properties

The nonlinear refractive index and nonlinear absorption coefficient of the PMMA before and after adding different concentrations of Rh6G ($1*10^{-5}$, $5*10^{-5}$, $1*10^{-4}$, $5*10^{-4}$ and $1*10^{-3}$) m/l were measured by the z-scan technique. The measurements were done at 1064 nm and 532 nm.

Nonlinear refractive index

To investigate the nonlinear refractive index, there are two wavelengths from the laser were chosen 1064nm and 532nm.Two energies were used to obtain the nonlinear refractive index of the PMMA before and after adding different concentrations of Rh6G and C480 dyes.

Concentration effect

The nonlinear refractive index of the dye-doped polymer thin film in different concentrations ($1*10^{-5}$, $5*10^{-5}$, $1*10^{-4}$,$5*10^{-4}$ and $1*10^{-3}$) m/l was measured by the z-scan technique. The measurements were done at 1064 and 532nm. Figs 19, 20 show a closed-aperture z-scan at different concentrations of Rh6G alone and with PMMA at wavelength 532nm, energy 33mJand 53mJ respectively.

Figs.21and 22 show a closed-aperture z-scan at different concentrations of Rh6G alone and with PMMA at wavelength 1064nm, energy 33mJ and 53mJ respectively.

Figs.23 and 24 show a closed-aperture z-scan at different concentrations of C480

alone and with PMMA at wavelength 532nm, energy 33mJ and 53mJ respectively.

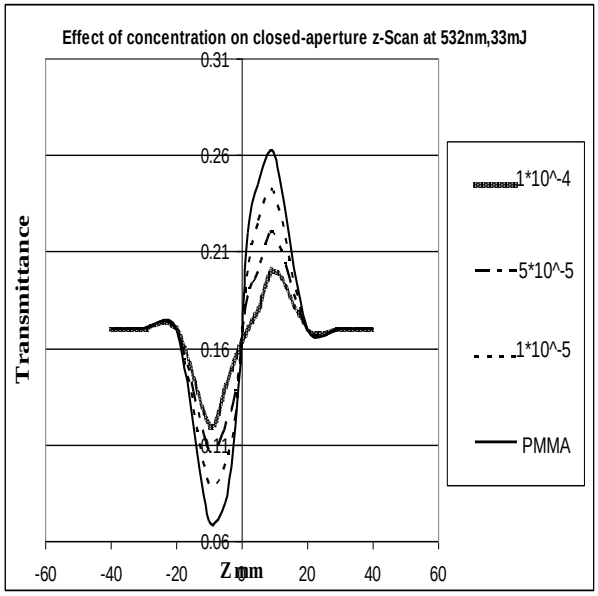

Fig.19: Effect of different concentrations of Rh6G and PMMA on closed-aperture z-scan at 532nm, 33mJ

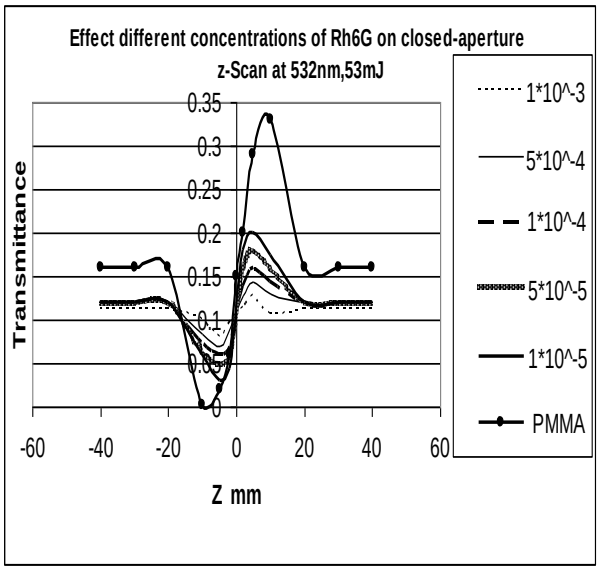

Fig.20: Effect different concentrations of Rh6G and PMMA on closed- aperture z-scan at 532nm, 53mJ

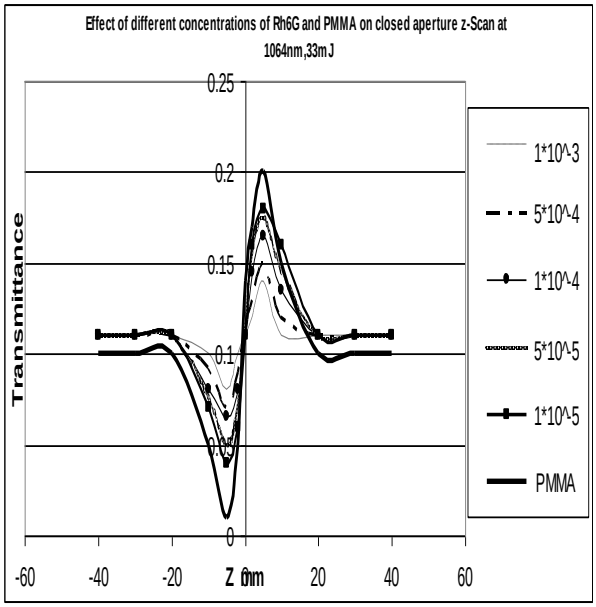

Fig.21: Effect of different concentrations of Rh6G and PMMA on closed-aperture z-scan at 1064nm, 33mJ

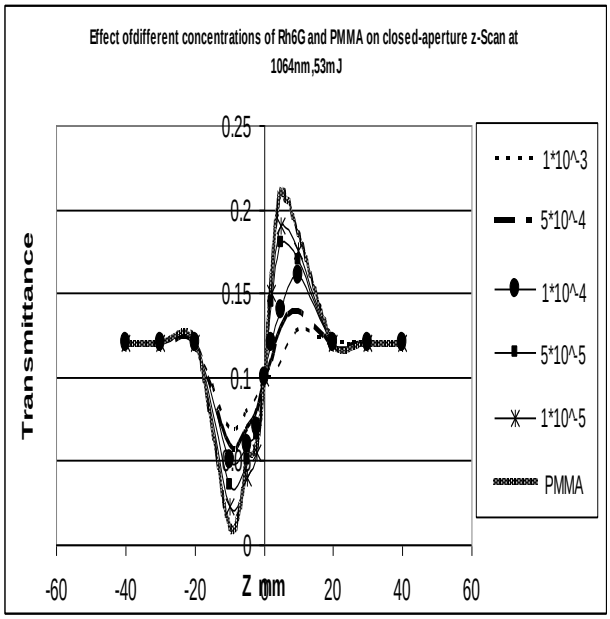

Fig.22: Effect different concentrations of Rh6G and PMMA on closed- aperture z-scan at 1064nm, 53mJ

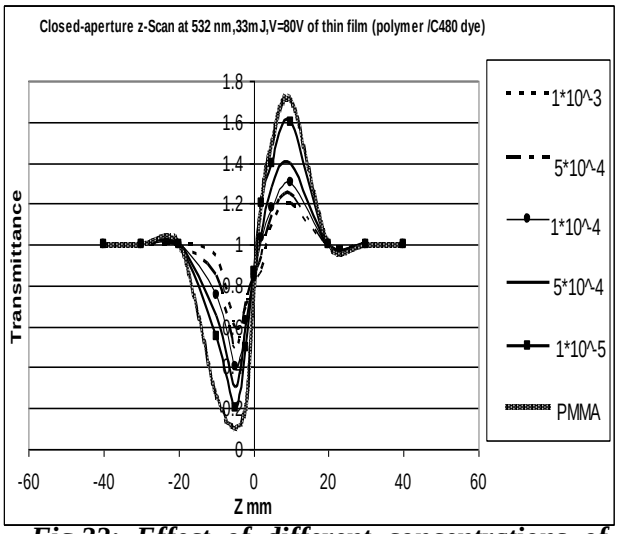

Fig.23: Effect of different concentrations of C480 and PMMA on closed-aperture z-scan at 532nm, 33mJ

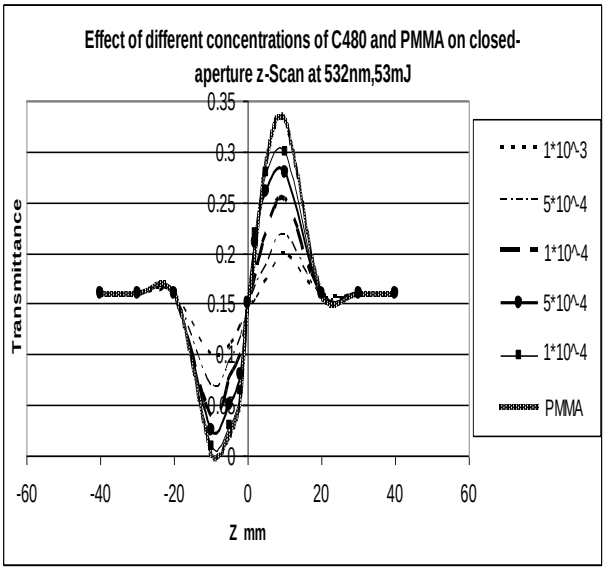

Fig.24: Effect of different concentrations of C480 and PMMA on closed- aperture z-scan at 532nm, 53mJ

Figs 25, 26 show a closed-aperture z-scan at different concentrations of C480 alone and with PMMA at wavelength 1064nm, energy 33mJ and 53mJ respectively.

Figs 19-26 have same behavior z-scan. The valley-peak configuration indicates the positive sign of n_2 .The scan started from distance far away from the focus, the beam irradiance is low. As the sample is brought closer to focus, the beam irradiance increases, leading to self-lensing in the sample.

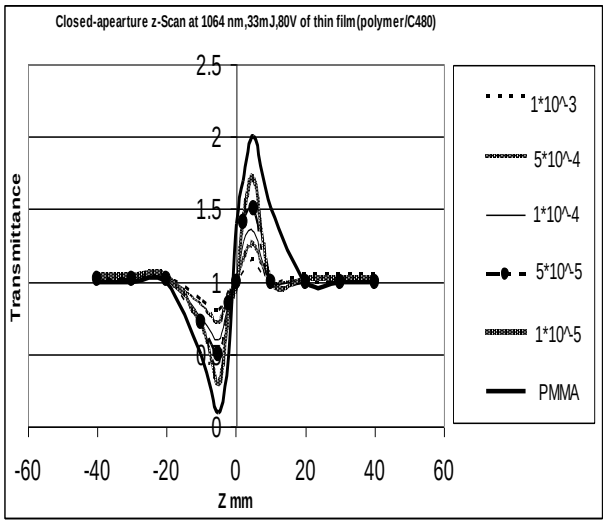

Fig.25: Effect of different concentrations of C480 and PMMA closed- aperture z-scan at 1064nm, 33mJ

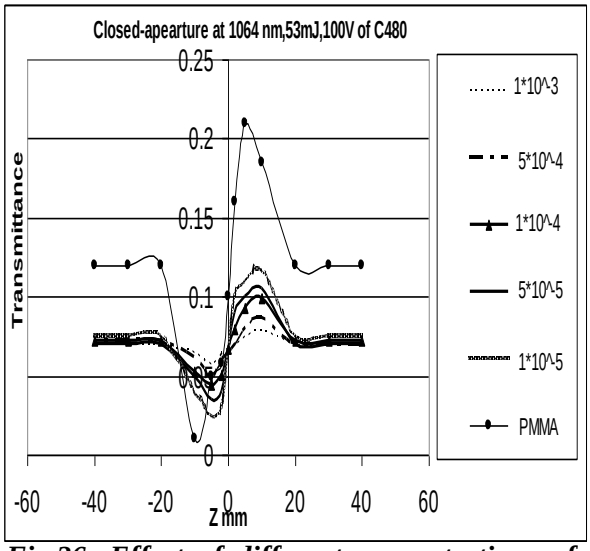

Fig.26: Effect of different concentrations of C480 and PMMA closed- aperture z-scan at 1064nm, 53Mj

The scan started with a linear behavior at different distances from the far field of the sample position (-Z) with respect to the focal plane at Z=0 mm. At the near field the transmittance begins to decrease until it reaches the minimum value (T_{Valley}) at approximately Z= -5mm or Z= -10mm.

Afterward, the transmittance begins to increase until it reaches the maximum value (T_{Peak}) at approximately Z=5mm or Z=10mm. Again, the transmittance begins to decrease toward the linear behavior at the far field of the sample position (+Z).

The behavior of z-scan curves was in good agreement with that obtained by Sheik-Bahae et al. [7], and N. Venkatram and Rao[13]. As results, the closed-aperture z-scan measures the change in transmittance of a beam, as the sample passes through the focal plane. The change in on-axis intensity is caused by self-focus or self-defocus by the sample as it travels through the beam waist[7]. This modified refractive index distribution then acts like a focusing lens. Hence, when the sample approaches to the focal plane, it will focus the converging beam more tightly. In the far field, this increases beam divergence and is measured as a decrease in energy through the aperture. At the focal plane, the divergence of the beam is unaffected by the sample and the detector measures no net change in transmittance. As it leaves the focal plane, the sample will focus the diverging beam. In the far field, this decreases beam divergence and is measured as an increase in power through the aperture.

A valley followed by a peak is the hallmark of a positive n_2. The peak to valley profile displayed in the figures, demonstrates the sample exhibited a self-focusing effect, i.e., it has a positive nonlinearity at 1064 nm and at 532 nm. The external self-focusing arising from the Kerr effect in Rh6G and C480-doped polymer thin film which appears in the peak and valley transmittance of each of z-scan trace.

The nonlinear refractive index is inversely proportional with increasing concentrations; the larger phase shift gives larger nonlinear refractive index. In addition, the magnitude of n_2 depends on the wavelength, but this dependence is not very strong at low pulse energy. In addition, the nonlinear refractive index was found to exhibit distinct behavior depending on the excitation pulse length. For short pulse length, at 532 nm, the magnitude of the nonlinear refractive index is independent of the pulse energy (Kerr nonlinearity); this property is more enhanced at 532 nm with the same results (but at less effect) at 1064 nm. In addition to this, the sensitivity of the experiment to refractive nonlinearities is entirely due to the aperture. The removal of the aperture will make the z-san sensitive to absorptive nonlinearities alone.

In all the closed-aperture curves, the peak to valley difference ΔT is between 0.022 - 1.4. In addition to this, the maximum and minimum transmittance occurred at Z equal to 10mm and -5mm or 10mm and -10 mm.

The closed-aperture z-scan defines variable transmittance values, which used to determine the nonlinear phase shift $\Delta\Phi_o$ using Eq.3 and the nonlinear refractive index at 532nm and 1064nm.

At first before added Rh6G or C480 to PMMA the magnitude of n_2 is larger when added the Rh6G or C480 to the polymer thin films is due to the Rh6G and C480 absorb visible light [14] and the interference between the polymer and Rh6G or C480 will cause scatter of the light. All these reasons will cause the refractive index will decrease when the addition of Rh6G or C480 to the PMMA [14].

The magnitude of n_2 is decreasing with increasing concentrations of Rh6G or C480.

In thermal effect the energy from the focused laser is transferred to the sample through linear absorption and is manifested in terms of heating the medium leading to a temperature gradient and there by the refractive index change across the sample which then acts as a lens. The phase of the propagating beam will be distorted due to the presence of this thermal lens [15].

Effect of the wavelength on nonlinear refractive index

To investigate the nonlinear refractive index, there are two wavelengths were chosen at 1064nm and 532nm.

The magnitude of n_2 depends on the wavelength, but this dependence is not very strong at low pulse energy. In addition, the nonlinear refractive index was found to exhibit distinct behavior depending on the excitation pulse length. For short pulse length, at 532 nm, the magnitude of the nonlinear refractive index is independent of the pulse energy (Kerr nonlinearity); this property is more effect at 532 nm with the same results (but at less effect) at 1064 nm.

Effect of the energy

In different concentrations of Rh6G and C480, the nonlinear refractive index at 33mJ is larger magnitude than nonlinear refractive index at 53mJ, where n_2 depends magnitude of nonlinearly-induced phase shift ($\Delta\Phi_o$) which in turn depends change in normalized transmittance between peak and valley (ΔTPV). The magnitude of n_2 starts with a small increasing at low input fluencies, at higher fluencies the value of n_2 decreased very strongly, the nonlinear refractive index is inversely proportional to the input energy.

The variation of n_2 is directly proportional to the input fluence, for low input fluence, the variation is high and showed approximately linear behavior, while at the higher fluencies this showed lower nonlinear refraction effect. Similar results were observed for pulse length at 1064 nm and at 532 nm. In contrast, the data measured at 532 nm and at 1064nm pulses show that n_2 increases with decreasing in the fluence. This variation may arise from such contributions as self-focusing of a sample. The nature of the nonlinear response can be inferred from its dependence on fluence.

Nonlinear absorption coefficient

To investigate the nonlinear absorption coefficient, there are two wavelengths were chosen 1064nm and 532nm. Two energies used to obtain the nonlinear absorption coefficient of the PMMA before and after adding different concentrations of R6G and C480 dyes.

Effect of the concentration

The addition of Rh6G or C480 to PMMA will change the nonlinear absorption coefficient of the polymer.

Figs 27 and 28 show open-aperture z-scan at different concentrations of Rh6G alone and with PMMA at 532nm, energy 33mJ and 53mJ respectively.

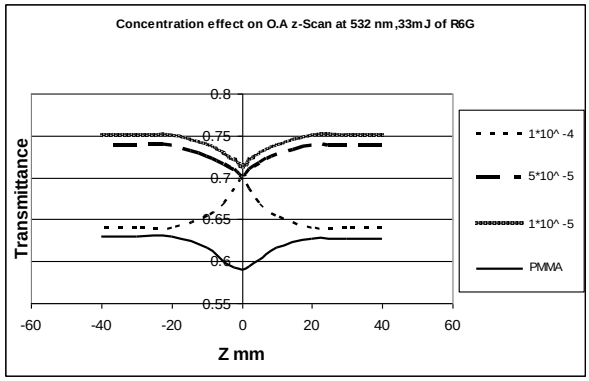

Fig.27: Concentration effect of Rh6G and PMMA on open-aperture z-scan at 32nm,33mJ

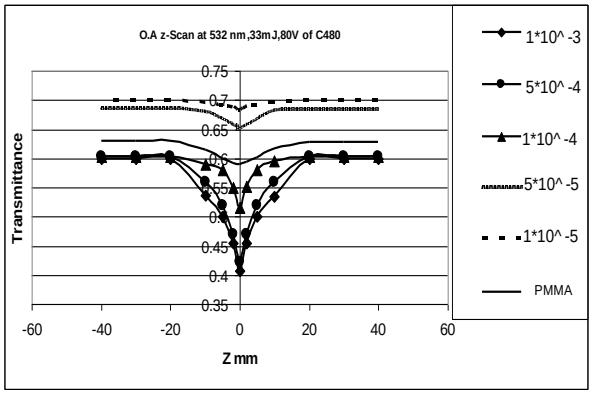

Fig.28: Concentration effect of Rh6G and PMMA on open-aperture z-scan at 532nm, 53mJ

Figs 29 and 30 show open-aperture z-scan at different concentrations of Rh6G

alone and with PMMA at 33mJ, 532nm, 1064nm respectively.

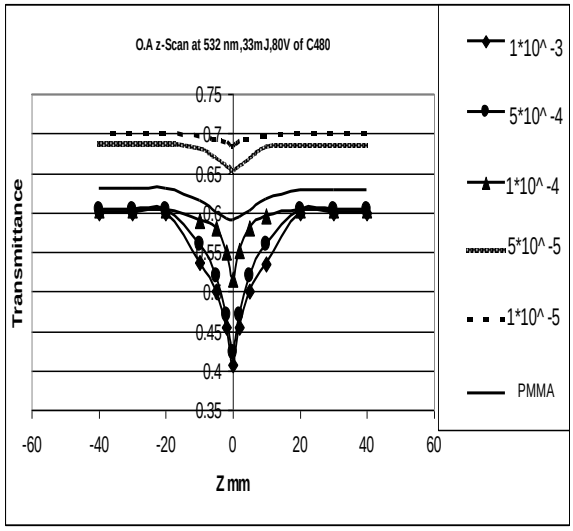

Fig.29: Concentration effect of Rh6G and PMMA on open-aperture z-scan at 532,33mJ

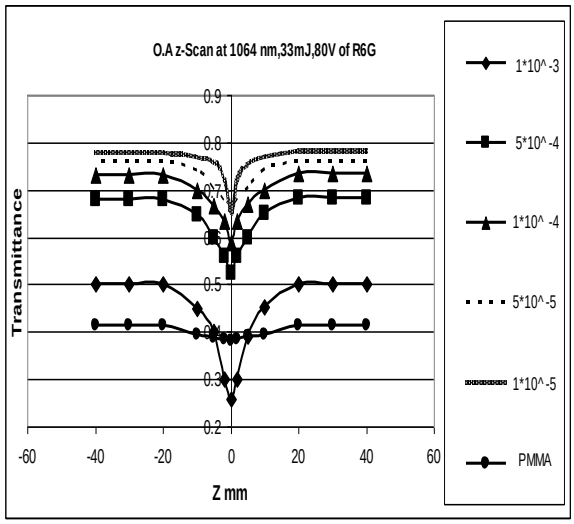

Fig.30: Concentration effect of Rh6G and PMMA on open-aperture z-scan at 1064nm, 33mJ

Fig. 31 shows open-aperture z-scan at different concentrations of Rh6G alone and with PMMA at 1064nm, 53mJ and Fig.32 shows open-aperture z-scan at different concentrations of C480 and with PMMA at 532nm, 33mJ.

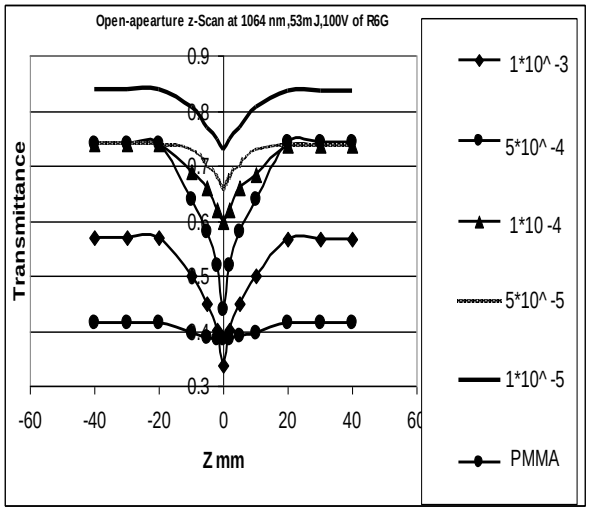

Fig.31: Concentration effect of Rh6G and PMMA on open-aperture z-scan at 1064nm, 53mJ

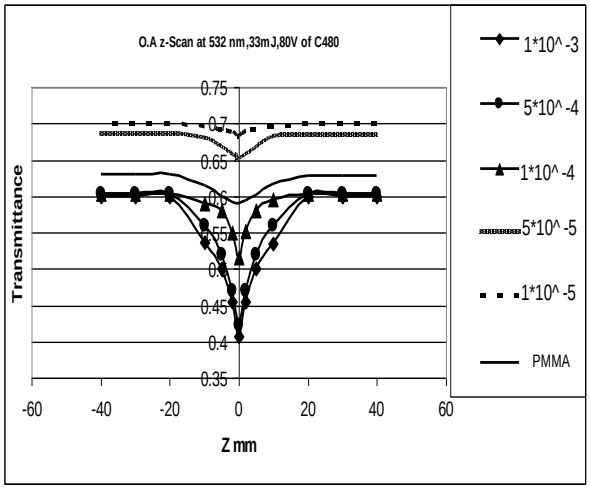

Fig. 32: Concentration effect of C480 and PMMA on open-aperture z-scan at 532nm, 33mJ

Fig.33 shows open-aperture z-scan at different concentrations of C480 alone and with PMMA at 532nm, 53mJ.

Figs.27-33 the behavior of transmittance started linearly at different distances from the far field of the sample position (-Z). At the near field the transmittance curve begins to decrease until it reaches the minimum value T_{min} at the focal point, where Z=0 mm.

Afterward, the transmittance begins to increase toward the linear behavior at the far field of the sample position (+Z).

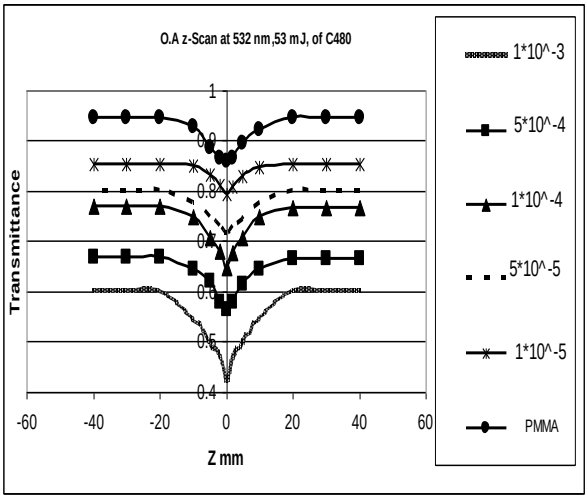

Fig.33: Concentration effect of C480 and PMMA on open-aperture z-scan at 532nm, 53mJ

The change of the intensity in this case is caused by two photon absorption(TPA) in the sample travels through beam waist ,that appear at the higher intensity on the experimental sample [16].

In polymer the change in intensity is caused by (TPA) while in dye-doped polymer with $1x10^{-4}$ M of Rh6G at 532nm, 33mJ the change in intensity is caused by saturable absorption [16].

In PMMA, the behavior of transmittance started linearly at different distances from the far field of the sample position (-Z). At the near field the transmittance curve begins to decrease until it reaches the minimum value (T_{min}) at the focal point, where Z=0 mm. Afterward, the transmittance begins to increase toward the linear behavior at the far field of the sample position (+Z). The change of the fluence in this case is caused by two photon absorption (TPA) in the sample travels through beam waist [16].

When Rh6G or C480 added to PMMA at 33mJ, the behavior of transmittance started linearly at different distances from the far field of the sample position (-Z). When Rh6G at concentration $1x10^{-4}$ M added to PMMA at 532nm, 33mJ, as shown in Fig.29 at the near field the transmittance curve begins to increase until it reaches the maximum value T_{max} at the focal point, where Z=0 mm. Afterward, the transmittance begins to decrease toward the linear behavior at the far field of the sample position (+Z). This behavior of nonlinear optical absorption response is demonated by saturable absorption. At high fluence in both wavelengths 532nm and 1064nm at 53 mJ the change in fluence is caused by (TPA) so the behavior of transmittance started linearly at different distances from the far field of the sample position (-Z). At the near field the transmittance curve begins to decrease until it reaches the minimum value T_{min} at the focal point, where Z=0 mm. Afterward, the transmittance begins to increase toward the linear behavior at the far field of the sample position (+Z).

The transmittance is sensitive to the nonlinear absorption as a function of input energy pulses. In PMMA the change in fluence is caused by (TPA) while in PMMA with $1x10^{-4}$ M of Rh6G at 532nm, 33mJ the change in fluence is caused by saturable absorption and with increase fluence to these composites at energy 53mJ the sample start showing two-photon absorption, since the TPA involves the absorption of two photons simultaneously the absorption is proportional to fluence [17]. In PMMA with $1x10^{-3}$ M and $5x10^{-4}$ M of Rh6G at 532nm, 33mJ the transmittance is not sensitive to the nonlinear absorption as a function of input energy pulses.

In the focal plane where the fluence is greatest, the largest nonlinear absorption is observed. At the far field of the Gaussian beam, where $|Z| >> Z_0$, the beam fluence is too weak to elicit nonlinear effects.

The open-aperture z-scan defines variable transmittance values, which used to determine absorption coefficient at 532nm.

Magnitude β starts with a large magnitude decreasing at low input fluencies, at higher fluencies the value of β decreased very strongly in PMMA when added Rh6G or C480 at 1064nm ,but at 532nm at 33mJ and 53mJ when added Rh6G the magnitude of β starts low in lower concentrations then increasing at high concentrations ,but in C480 at 532nm at 33mJ and 53mJ the magnitude of β starts high at lower concentrations then decreasing at high concentrations ,where both them(Rh6G and C480) absorb the visible light but in different degrees dependence on kind of material, so these will change the nonlinear absorption coefficient.

Conclusions

The following remarks are concluded during the present work:

- For thin film (PMMA+C480) the nonlinear absorption coefficient is directly proportional to the input fluence which caused by self defocusing of the material and directly proportional to the increasing in the concentration of the dye due to the thermal effect in the film sample.
- For thin film (PMMA+Rh6G) the nonlinear absorption coefficient is inversely proportional to the input energy and directly proportional to the increasing in concentration of the dye, the nonlinear absorption coefficient of PMMA is caused by the effect of two photon absorption, at 532nm Rh6G at $1x10^{-4}$ M added to the polymer the nonlinear absorption coefficient at the low fluence is caused by the saturable absorption.
- For both thin films (PMMA+C480) and (PMMA+Rh6G) the nonlinear refractive index is inversely proportional to the input energy.
- The nonlinear refractive index is more affected at the wavelength 532 nm than at 1064 nm.
- The nonlinear absorption coefficient is more affected at the wavelength 1064 nm than at 532 nm.
- For thin film (PMMA+C480) increasing the wavelength leads to decreasing the difference in normalized transmittance from peak to vally phase shift (ΔTPV).

References

[1] T.Y. Tou et al., J. Opt. Mater, 4, 29 (2005) 963-969.

[2] R.P. Haugland, "Handbook of Fluorescent Probes and Research Chemicals", 7th ed., (Molecular Probes, Eugene, OR), 1999.

[3] U. Brackmann, "Lambdachrome Laser Dyes ", 2nd. ed., (Lambda Physik,. Göttingen), (1994) 198–199.

[4] S. V. Rao, N. K. M. Naga srinivas, and D. N. Rao, " Nonlinear absorption and excited state dynamics in Rhodamine B studied using Z-scan and degenerate four wave mixing techniques", Chem. Phys. Lett., 361 (2002) 439-445.

[5] M. Sheik-Bahae and M. P. Hasselbeck , OSA Handbook of Optics,Vol. IV, Chapter 17, (2000).

[6] X. C. Peng, T. Jia, J. P. Ding, J. L. He and H. T. Wang, Optical Sociaty of American, 22, 2 (2005) 446-452.

[7] M. Sheik-Bahae, A. A. Said, T. Wel, D. J. Hagan and E. W. Van, "IEEE J. of Quantum Electronic, 26, 4 (1990) 760-769.

[8] Y. Wang, M. Saffman, Opt. communications, 241, 66 (2004) 513-520.

[9] F. I. Ezema, Turk. J. Phys., 22, 29 (2005) 105 - 114.

[10] R. Philip and G. R. Kumar, The American Physical Society, 62, 19 (2000) 169-194.

[11] R. de Nalda, R. del Coso, J. Requejo-

Isidro, J. Olivares, A. Suarez-Garcia, J. Solis and C. N. Afonso, Nalda., 19, 178 (2002) 123-126.
[12] J.F. Ready, "Industrial Application of Lasers", 2nd, Academic Press, San Diego, (1978).
[13] N. K. Venkatram and D. N. Rao, Optical Society of America, 13, 22 (2005) 867-872.
[14] L.G. Carotenuto "Metal Polymer Nanocomposite", Wiley Interscience publication, New Jersey. (2004)
[15] Gonli et al., Opt. Express 13, 20 (2005) 1-13.
[16] I. Polyzos, G. Tsigaridas, M. Fakis, V. Giannetas, P. Persephonis, J. Mikroyannidis, Chem. Phys. Lett., 369 (2003) 264.
[17] N. Venkatram, R. S. S. Kumar, D. N. Rao, S. K. Medda, S. De and G. De., Journal of Nanoscience and Nanotehnology, 28, 6 (2006) 1-5.